JOURNAL OF Applied Polymer SCIENCE

Blending chitosan-g-poly(caprolactone) with poly(caprolactone) by electrospinning to produce functional fiber mats for tissue engineering applications

Dominik de Cassan,[1] Alexander Becker,[2,6] Birgit Glasmacher,[2,6] Yvonne Roger,[3,6] Andrea Hoffmann,[3,6] Thomas R. Gengenbach,[4] Christopher D. Easton,[4] Robert Hänsch,[5] Henning Menzel [1]

[1]Technische Universität Braunschweig, Institute for Technical Chemistry, Braunschweig, Germany
[2]Institute for Multiphase Processes, Gottfried Wilhelm Leibniz Universität Hannover, Hannover, Germany
[3]Department of Orthopedic Surgery, Hannover Medical School, Graded Implants and Regenerative Strategies, Hannover, Germany
[4]CSIRO Manufacturing, Clayton, Australia
[5]Technische Universität Braunschweig, Institute of Plant Biology, Braunschweig, Germany
[6]Lower Saxony Centre for Biomedical Engineering, Implant Research and Development (NIFE), Hannover, Germany
Correspondence to: H. Menzel (E-mail: h.menzel@tu-braunschweig.de)

ABSTRACT: Use of electrospun fiber mats for tissue engineering applications has become increasingly prominent. One of the most important polymers in research, poly(ε-caprolactone) (PCL), however, lacks biological performance, easy access to modifications and cellular recognition sites. To improve these properties and to enable further modifications, PCL was blended with chitosan grafted with PCL (CS-g-PCL) and subsequently processed via electrospinning. In this way, chitosan was enriched at the fiber's surface presenting cationic amino groups. The fiber mats were analyzed by various techniques such as scanning electron microscopy (SEM), confocal laser scanning microscopy (CLSM), and X-ray photoelectron spectroscopy (XPS). Furthermore, analyzing thermal properties and crystallinity, showed that an increased content of CS-g-PCL in blend composition leads to a higher overall crystallinity in produced fiber mats. Blending CS-g-PCL into PCL significantly increased initial cellular attachment and proliferation as well as cell vitality, while maintaining adequate mechanical properties, fiber diameter, and interstitial volume. As proof of principle for easy access to further modification, fluorescently labeled alginate (Alg-FA) was attached to the fiber's surface and verified by CLSM. Hence, blending CS-g-PCL with PCL can overcome an inherent weakness of PCL and create bioactive implants for tissue engineering applications. © 2019 The Authors. *Journal of Applied Polymer Science* published by Wiley Periodicals, Inc. J. Appl. Polym. Sci. **2020**, *137*, 48650.

KEYWORDS: Blend; cell compatibility; chitosan; electrospinning; polycaprolacton; surface enrichment; X-ray photoelectron spectroscopy

Received 20 June 2019; accepted 10 October 2019
DOI: 10.1002/app.48650

INTRODUCTION

In the past decades electrospinning has become an established technique to produce scaffolds for biomedical applications[1,2] such as tissue repair, wound dressings, controlled drug carriers and implants.[3–5] These electrospun constructs offer various advantages such as a high surface area and are able to mimic the structure of extracellular matrix (ECM). Due to its versatility and easy access to modification of processing parameters, electrospinning can produce scaffolds of various morphologies, fiber diameters, and porosity, which are all critical parameters for a later application *in vivo*.[2,4]

Polycaprolactone (PCL) is a biodegradable and biocompatible polyester, which shows adequate mechanical properties[3,4,6] to be used as a potential implant bridging complex tissue transitions such as tendon to bone junctions.[7] However, because of its hydrophobic nature and its lack of natural cell recognition sites its use in biomedical applications is limited.[8–10] Various approaches such as plasma treatment,[9] wet chemical modification[10] or coating with graft-copolymers, such as chitosan-graft-polycaprolactone (CS-g-PCL),[11] were developed to overcome these weaknesses. Blending of PCL with other polymers offers an easy and economical alternative to modification methods and treatments of already spun fibers.[12]

CS is a natural polymer produced from shrimps or fungi and is known for its excellent biocompatibility.[13] Furthermore, previous studies highlighted its antibacterial and wound healing properties.[14] Its use in tissue engineering applications, however, is limited, since chitosan itself is not only very hard to process by electrospinning, mainly due to its insolubility in common organic

solvents, but also results in highly brittle, mechanically weak fibers once processed.

In recent studies, it was shown that coating of electrospun PCL scaffolds with CS-g-PCL graft-copolymers resulted in highly biocompatible scaffolds for potential tissue engineering applications.[7,15] In the coating, the PCL grafts were crystallizing onto the PCL nanofibers and the chitosan was presented at the surface, offering various advantages such as cell recognition sites and a surface charge available for subsequent modification.[7,16] However, modification involved a multistep process with coating, drying, and washing. An easier and more direct method to functionalize electrospun fibers would be directly blending PCL with CS-g-PCL in the spinning process. Blending is well established in the field of electrospinning as well as the fact that blending of polar additives to a nonpolar matrix in the electrospinning process may result in an enrichment of polar groups at the fibers' surface.[17,18] Therefore, it could be expected to find the polar chitosan moieties of CS-g-PCL at the fiber surface and the blending of CS-g-PCL in the electrospinning process should result in a similar fiber surface as a modification without the necessity of additional process steps. Blending can be expected to yield fibers, which show the same improved properties regarding surface functionalities and biocompatibility,[15,19] while the deposition of drug-delivery systems or biopolymers should be possible on these surfaces.[7] A serious consideration that requires careful examination is that blending can strongly affect processing parameters, degradation behavior, and material properties of fibers.[20]

In this study, we used blends of PCL and CS-g-PCL to prepare biocompatible scaffolds by electrospinning. The scaffolds were evaluated regarding their composition (NMR), properties (SEM, mechanics, porosity), and potential enrichments of polar functionalities at the fiber surface (XPS, CLSM). Furthermore, samples were analyzed toward their thermal properties and crystallinity (DSC) as well as cytocompatibility with human mesenchymal stromal cells (MSC).

MATERIALS AND METHODS

Materials

Unless otherwise stated all chemicals used were purchased from Sigma-Aldrich. PCL (M_n = 80 000) and chitosan (M_n = 110 000-150 000, degree of deacetylation 83% according to ^{1}H-NMR) were purchased from Sigma as well. 2,2,2-Trifluoroethanol was purchased from ABCR (Karlsruhe, Germany).

Synthesis of CS-Graft-PCL. Synthesis of chitosan-graft-polycaprolactone (CS-g-PCL) was carried out according to known procedures.[7,16] Dry chitosan (350 mg, 2.09 mmol, 83% degree of deacetylation according to ^{1}H-NMR) was dissolved in $MeSO_3H$ (2 mL) in a flame-dried 50 mL Schlenk-flask equipped with a magnetic stirrer under nitrogen atmosphere for 1 h at 45 °C. After the chitosan was completely dissolved, ε-caprolactone monomer (3.98 mL, 42.12 mmol, 18 eq.) was added and stirred under nitrogen atmosphere for 5 h at 45 °C. Subsequently, 43.75 mL of 0.2 M KH_2PO_4, 7 mL of 10 M NaOH and 100 mL of ice were added to the reaction mixture under vigorous stirring. The precipitated raw CS-g-PCL (1:18) was collected by vacuum filtration, washed with deionized water, and vacuum dried for 24 h. The crude CS-g-PCL was dissolved in N,N-dimethylformamide, reprecipitated in H_2O, and vacuum dried again.

Synthesis of Alginate-Fluoresceinamine. Synthesis of fluorescently labeled alginate (Alg-FA) was carried out according to de Cassan *et al.*[7] Alginate (21 eq.) was dissolved in 2-(*N*-morpholino) ethanesulfonic acid (MES)-buffered solution (0.5 M pH = 5.45). 1-Ethyl-3-(3-dimethylaminopropyl)carbodiimid hydrochloride (2 eq.) and N-hydroxysuccinimide (2 eq.) were dissolved in MES buffered solution as well. Subsequently the solutions were combined and stirred for 30 min. Fluoresceinamine (FA) (1 eq.) in MES was added dropwise, and the reaction mixture was stirred for 48 h at room temperature. Subsequently the mixture was filtered and dialyzed against deionized water. After lyophilisation, the sample was characterized by ^{1}H-NMR spectroscopy. The degree of modification DM_{FA} was calculated according to ^{1}H-NMR and amounts to 1.3%.

Electrospinning of PCL/CS-g-PCL Blends. Ten different blends, with the PCL content varying from 10 to 90% (w/w) were processed. Solutions containing 170 mg of PCL per mL of 2,2,2-trifluoroethanol (TFE) and 1000 mg of CS-g-PCL per mL of chloroform served as source materials. All experiments were performed at room temperature. Samples were mixed overnight by shaking. Pure PCL and CS-g-PCL were processed to create a reference within this study. The electrospinning device consisted of a syringe holding the blends, an emitter connected by polyethylene tubing, and a collector covered with aluminum foil.[21] Due to the need of aligned fibers for mechanical testing, samples for mechanical testing were produced using a drum collector with a rotational speed of 8 m/s. The remaining parameters were set to 20 cm emitter to collector distance, 20 kV voltage, 4 mL/h flow rate, and a process time of 90 min. All other samples were spun on an aluminum foil covered plate collector with an emitter to collector distance of 25 cm, voltage set to 20 kV, flow rate of 4 mL/h, and process times of 30 min each.

Modification of Fiber Mats with Alg-FA. Fiber mats were modified by immerging them into a solution of Alg-FA dissolved in deionized water (2 mg/mL) for 2 min. Subsequently the samples were washed in deionized water 5 times for 2 min each and dried in vacuum overnight.

Characterization Methods

^{1}H-NMR spectra of the samples were recorded on a *BRUKER* AV II-300 (Rheinstetten, Germany) (300 MHz) at 25 °C using deuterated $CDCl_3$ as solvent with tetramethyl silane as internal reference.

To determine fiber diameters, SEM images were taken (S-3400 N, Hitachi). These SEM images were analyzed with image analysis software (AxioVision, Carl Zeiss). A diagonal line was drawn into each picture. All fibers crossing this line were, on both sides of the line, examined at least four times regarding their diameter to calculate average fiber diameters.

Contact angle measurements were carried out with a *DATAPHYSICS* Type OCA 15 (Filderstadt, Germany) using the sessile drop method. Nine microliters of bidestilled water were brought to the sample surface and the contact angle was probed using a camera for online data processing (SCA 20 software by *DATAPHYSICS*). Each sample was measured at least 9 times to determine the average.

Confocal Laser Scanning Microscopy (CLSM) was carried out on a ZEISS CLSM-510 Meta scan head connected to a Zeiss Axiovert

200 M (Oberkochen, Germany). Samples were measured at least three times to verify the results, and wavelength scans were performed to prove that measured signals did not result from reflection but from fluorescence. Zen Blue Imaging software (ZEISS) was used to determine the mean fluorescence of samples. To do so, images were separated into squares of 10 000 μm^2 and analyzed for their mean fluorescence to calculate the average values in arbitrary units (a.u.).

Differential scanning calorimetry (DSC) measurements were carried out on a Netzsch DSC204 Phoenix connected to Netzsch TASC 414/3A controller equipped with a CC-200 cooling controller from Netzsch (Selb, Germany). Fiber mats produced from PCL blends were sealed in alumina pans with a pierced lid and exposed to a double heat cycle. Samples were heated up from room temperature to 120 °C with a heat rate of 10 °C/min. Subsequently, the samples were cooled down to −100 °C with a cooling rate of 10 °C/min and heated up again to 120 °C with 10 °C/min. The same procedure was applied to mixed but unprocessed polymers as well. Proteus thermal analysis software (Netzsch) was used to quantify melting temperature (T_m), enthalpy of fusion (H_{FUS}), glass transition temperature (T_g), and change in heat capacity at glass transition (ΔC_p).

Capillary Flow Porometry was carried out on a Quantachrome Instruments Porometer 3Gzh (Boynton Beach, Florida). Fiber mat samples of 25 mm diameter were wetted with Porofil Porometer Wetting Fluid (Boynton Beach, Florida) and each tested within a wet and a dry cycle. 3GWin2 software (Quantachrome Instruments) was used to determine minimum, mean, and maximum pore size.

Static tensile testing was carried out using a universal testing machine (5655, Instron). The specimens were mounted in dry state onto the universal machine using pneumatic grips and tested at room temperature with a crosshead speed of 40 mm × min^{-1} and 500 N load cell. All specimens were stretched until failure. The used specimens were deposited on a rotating drum collector. This leads to circumferentially aligned fibers. During load application, in a first step, nonaligned fibers will be straightened, however, this fiber rearrangement prevents recording of reasonable data for forces and elongation. To avoid these effects due to changing the materials properties during the process, static tensile testing has to be performed on aligned specimens. However, all other test methods were carried out with nonaligned fiber mats.

X-ray photoelectron spectroscopy (XPS) analysis was performed on an AXIS NOVA spectrometer (Kratos Analytical Inc., Manchester, UK) using a monochromatic Al K_α source at a power of 180 W (15 kV × 12 mA) with a hemispherical analyzer in the fixed analyzer transmission mode and the standard aperture (~0.3 × 0.7 mm analysis area). Total pressure in the main vacuum chamber was between 10^{-9} and 10^{-8} mbar. Survey spectra were acquired with a pass energy of 160 eV. To obtain detailed information about chemical structure and binding states, high-resolution spectra were recorded from individual peaks at 20 or 40 eV pass energy. The specimens were analyzed at an emission angle of 0° as measured from the surface normal. XPS analysis depth ranges between 5 and 10 nm for a flat surface assuming typical values for electron attenuation length of relevant photoelectrons. In the case of rough surfaces (as in this study), the actual emission angle varies between 0° and 90° and, consequently, sampling depth may range from 0 nm to approximately 10 nm. Data processing was performed using CasaXPS processing software (Casa Software Ltd., Teignmouth, UK). All elements present were identified from survey spectra. Atomic concentrations were calculated using integral peak intensities and sensitivity factors for the respective elements supplied by the manufacturer. Binding energies were referenced to the C 1 s peak at 285 eV for aliphatic hydrocarbon. Accuracy of quantitative XPS measurements is approximately 10–15%, however precision depends on signal/noise ratio and is usually much better than 5%. This is relevant when comparing similar samples as performed in this study.

Human bone marrow MSCs were cultivated in DMEM (FG0415, Biochrom) plus supplements (10% FCS Hyclone, Thermo Fisher Scientific, not heat-inactivated; 25 mM 4-(2-hydroxyethyl)-1-piperazineethanesulfonic acid (HEPES) buffered solution (Biochrom; 100 U/mL penicillin/100 µg/mL streptomycin, Biochrom; 2 ng/mL recombinant human FGF-2 [*Escherichia coli*], Peprotech) in a T300 tissue culture flask (TPP) until they reached a 70–80% confluency. After detaching the cells with 0.05% trypsin/0.02% EDTA (Biochrom), they were seeded onto the scaffolds with a density of 10.000 cells per cm^2. The cultivation was performed at 37 °C and 5% CO_2.

The preparation of the scaffolds and the well plates for cell culture was described previously.[7] In brief, 48-well plates were treated with 100 µL polyHEMA (poly- (2-hydroxyethyl methacrylate, Sigma) solution (0.02 mg/mL polyHEMA in 1:1 acetone/ethanol) for 10 min at room temperature. After removing the solution and evaporation of residual solvents in a safety cabinet, the wells were washed twice with phosphate-buffered saline (PBS) and once with DMEM plus supplements. The scaffolds were washed with 70% ethanol for 30 min at room temperature and sterilized via UV-light for 30 min on each side. Finally, the scaffolds were washed three times with PBS and once with DMEM plus supplements.

The viability of the cells was studied by using the Colorimetric Cell Viability Kit I (based on WST-8 [(2-(2-methoxy-4-nitrophenyl)-3-(4-nitrophenyl)-5-(2,4-disulfophenyl)-2H-tetrazolium, monosodium salt], Promokine). Cells were cultivated for 1 day, 3 days, and 7 days. Used media was replaced with fresh media and mixed with the WST-8 solution in a 1:10 dilution. After incubation for 4 h at 37°C with 5% CO_2, the absorbance of the supernatant was quantified at 450 nm (OD_{450}). The cells were washed with PBS and further incubated with DMEM plus supplements.

RESULTS AND DISCUSSION

To improve electrospun PCL fiber mats for biomedical applications, blending of PCL with polymers like CS appears promising but is challenging to implement successfully. According to the literature, the CS amino groups should enrich at the fibers' surface[17] and therefore improve cell adhesion[7,15] and allow to deposit drug-delivery systems.[7,22] However, the compatibility of PCL with CS is low.[23,24] Therefore, we prepared a CS-g-PCL copolymer, which should allow miscibility and concomitantly phase separation and surface enrichment.[24,25]

Synthesis

We synthesized CS-g-PCL copolymers according to the literature[7] by grafting ε-caprolactone onto the hydroxyl groups of CS

by ring-opening polymerization. Methanesulfonic acid acted as solvent and catalyst. As published in our previous studies,[7] using 2D NMR experiments it was shown that the reaction occurs mainly on the primary alcoholic function of CS. Here, an exemplary 1D NMR is shown in Figure 1, which can be used to determine the ratio of PCL units to glucosamine units.

The spectrum is in line with previous reports and the ratio of the integrated signals **e** or **c** (2 protons) and signal **3** (1 proton) indicated a composition of the graft polymer with 18 PCL units per glucosamine unit.

Evaluation of Electrospun Scaffolds

To obtain a systematic overview regarding the properties of PCL blended with CS-g-PCL and subsequently processed by electrospinning, a broad range of compositions was prepared. As a control group, PCL was processed with slightly adapted parameters known from the literature[7] and analyzed subsequently. Furthermore, samples with increasing amounts, in steps of 10% (w/w) each, of the second blend component, CS-g-PCL, were prepared. To do so, both polymers were dissolved in solvents to create solutions with a medium to high viscosity, which are applicable to electrospinning processes. While PCL is soluble in various organic solvents such as trifluoroethanol (TFE), CS-g-PCL is more difficult to dissolve in high concentrations and necessary viscosities, which is mainly due to its hydrophilic and hydrophobic parts. It was found that CS-g-PCL is highly soluble in chloroform ($CHCl_3$), which is a suitable solvent for electrospinning due to its volatility[26] and that CS-g-PCL can be dissolved in such a way that a high viscosity is reached, which is beneficial for a stable electrospinning process. After dissolving both polymers alone, various amounts of CS-g-PCL solution were added to PCL solution to create desired blend compositions. Since the highly viscous CS-g-PCL was transferred to the PCL solution, it is possible that the transfer was not carried out completely. Therefore, the final composition of produced blends was measured via ^{1}H-NMR. Furthermore, the various blend compositions proceed with different solvent ratios, different viscosities, and processabilities. These could affect material properties of the produced fiber mats such as fiber diameter, interstitial volumes, or crystallinity properties.[26] To compare produced fibers, the same electrospinning setup as for pure PCL fibers was used. This setup allowed manufacturing of reproducible fibers in a stable electrospinning process.

After electrospinning, scaffolds were analyzed using ^{1}H-NMR to evaluate the content of graft-copolymer in the processed material. As shown in Figure 2, the theoretical proportion of PCL to CS-g-PCL differed from the desired proportion in the processed scaffolds. The intended sample composition was not achieved, with a higher amount of PCL found in most samples. During the preparation step, CS-g-PCL solution was transferred into a PCL solution and mixed subsequently. This discrepancy is likely due to high viscosity of the polymer solutions, which is required for a stable electrospinning process. However, *via* NMR measurements the exact composition of scaffolds could be determined and was used for subsequent analytics.

To determine fiber diameter and fiber morphology, SEM measurements of produced fiber mats were performed. It was observed that an increasing content of graft-copolymer did not change the fiber morphologies over a very broad range of blend compositions (0–80% (w/w) CS-g-PCL) (see Figure 3). However, using very high amounts of CS-g-PCL (90% (w/w)) led to more strongly matted fibers, which was not expected. CS-g-PCL was dissolved in chloroform and due to the higher volatility of chloroform compared to TFE the electrospinning solution should evaporate faster. This should result in a deposition of completely dried fibers on the electrospinning collector and avoid matting of the fiber mats due

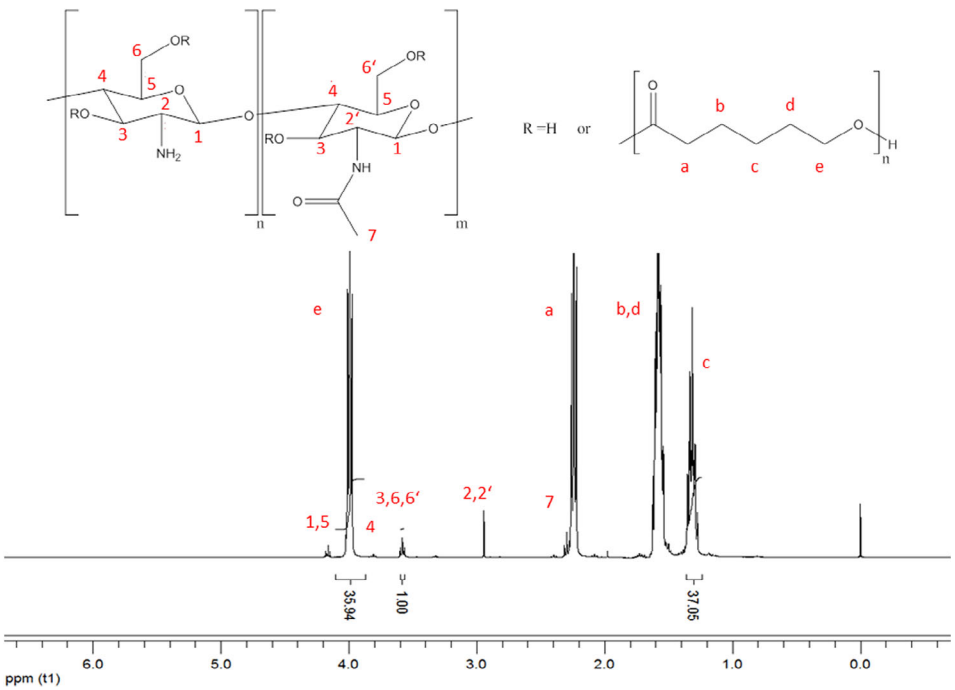

Figure 1. ^{1}H-NMR spectra of CS-g-PCL$_{18}$ copolymer. [Color figure can be viewed at wileyonlinelibrary.com]

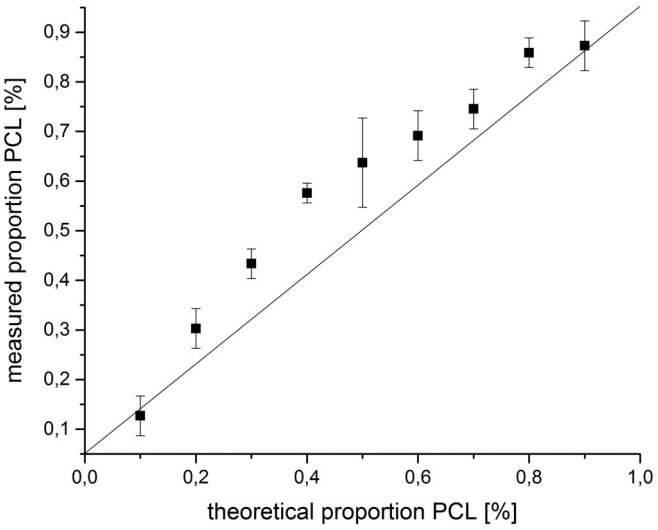

Figure 2. Theoretical and measured proportions of PCL in processed blends after electrospinning ($n \geq 3$, SD).

to remaining solvent. However, apart from the volatility other parameters such as viscosity have an effect on electrospinning processes[26,27] and could explain the matted fibers. This stronger fusion of fibers is not necessarily a negative outcome, because potentially it can improve mechanical strength. To evaluate the fiber mats further, fiber diameters were determined.

As shown in Figure 4, it was observed that fiber diameter remained unchanged over almost the complete range of blends, which was further supported by their constant fiber morphology. The fibers showed a diameter of around 1 ± 0.35 µm. However, compositions consisting of 90% (w/w) CS-g-PCL showed a significant increase in fiber diameter up to 2.04 ± 0.41 µm. This could be due to the change in solvent ratio and viscosity. While PCL was dissolved in TFE, CS-g-PCL was dissolved in chloroform, which evaporates faster and has a different viscosity compared to TFE. This increase in fiber diameter could lead to a decrease in interstitial volume, which would not necessarily be beneficial for cellular ingrowth and support.[1,28]

Interstitial volume, simplistically named pore size, was evaluated using intrusion porometry. However, no significant change in pore size and distribution was found (Table I). Unfortunately, blends with compositions of 90% (w/w) CS-g-PCL were too brittle to be measured. This fact together with general handling of these samples showed, that this composition is not applicable for later use as an implant and therefore not been evaluated in detail any further. Taken together, all relevant blend compositions showed comparable pore sizes and should be equivalently qualified for relevant parameters such as cell ingrowth or nutrient support.

Electrospun blends were evaluated regarding their wettability. This is an important parameter for potential cell response to the surface. The water contact angle was evaluated using sessile drop method at room temperature by measuring the angle between a water droplet and sample surface. PCL fiber mats showed a contact angle of 127 ± 3°, which confirmed the hydrophobic nature of PCL. The contact angle for flat PCL surfaces is 81°.[29] However, the contact angle is not only defined by the surface chemistry but also by topography. Rough hydrophobic and rough hydrophilic surfaces show more extreme contact angles compared to smooth surfaces of the same material.[30] This effect may also result in a sudden change from very large contact angles to complete wettability.[31] The PCL fiber mats did not have a smooth surface, but a rough and irregular surface topography, thus the higher contact angle compared to the smooth PCL is in line with the structure. By blending PCL with CS-g-PCL, the surface wettability should increase due to the presence of hydrophilic CS at the fiber surface and its hydroxy and amine groups. Measurements showed that all fiber mats prepared with blends showed full wettability, already 10% (w/w) of CS-g-PCL were sufficient to obtain fiber mats, which showed a contact angle of 0°. This good wettability was considered as favorable for cell adhesion.[32]

Thermal Properties and Crystallinity

DSC is a fast and straightforward method to determine thermal properties and crystallinity, which are critical for later application and might strongly influence the materials' mechanical properties or degradation behavior. A double heating cycle was applied for the samples as described previously to determine samples actual crystallinity (first heat cycle) and its ability to crystallize (second heat cycle).[33] Unless otherwise stated, all data depicted here are from the first heat cycle and hence indicate samples actual crystallinity. The thermograms for processed, namely electrospun, and unprocessed materials differ. The processed material showed a single, rather broad melting peak indicating that the blends consist of only one, more or less homogenous, crystalline phase. However, the large width of the melting peak indicates that this phase consists of a distribution of various crystalline states. This might be due to the electrospinning process itself, which leads to a phase separation resulting in "pure" PCL phases and phases of graft-copolymer during the drying process of the fibers. Such processes of enrichment of certain phases are well known in the literature.[17] The unprocessed materials however showed two melting peaks, indicating two distinct crystalline phases. Since the unprocessed materials were not dissolved and mixed afterward but just ground and mixed in a solid state, it is likely that they did not form a homogeneous blend. The processed materials, however, were both dissolved in solvents and mixed subsequently in the liquid phase, which should facilitate the formation of a good blend and phase reorganization.[25,34] The double melting peak in unprocessed material could result from pure PCL and the PCL containing graft-copolymer consisting of PCL chains in different phases or structural compositions. This could be due to PCL and CS-g-PCL differing in their ability to crystallize and resulting crystal size. PCL as a linear polymer chain should be able to crystallize easily at higher temperatures and form crystallites with a high lamellae thickness in contrast to the branched and relatively poor ordered CS-g-PCL; this probably resulted in the observed double melting peaks on DSC thermograms.[35] The second lowered melting peak can be explained, even without any effects of reorganizational or matrix effects, with the increase of components hardly crystallizing in the actual blend, which result in a lower overall intermolecular interaction.[36]

By blending CS-g-PCL into PCL, the resultant material properties could differ. Materials' enthalpy of fusion, change in heat

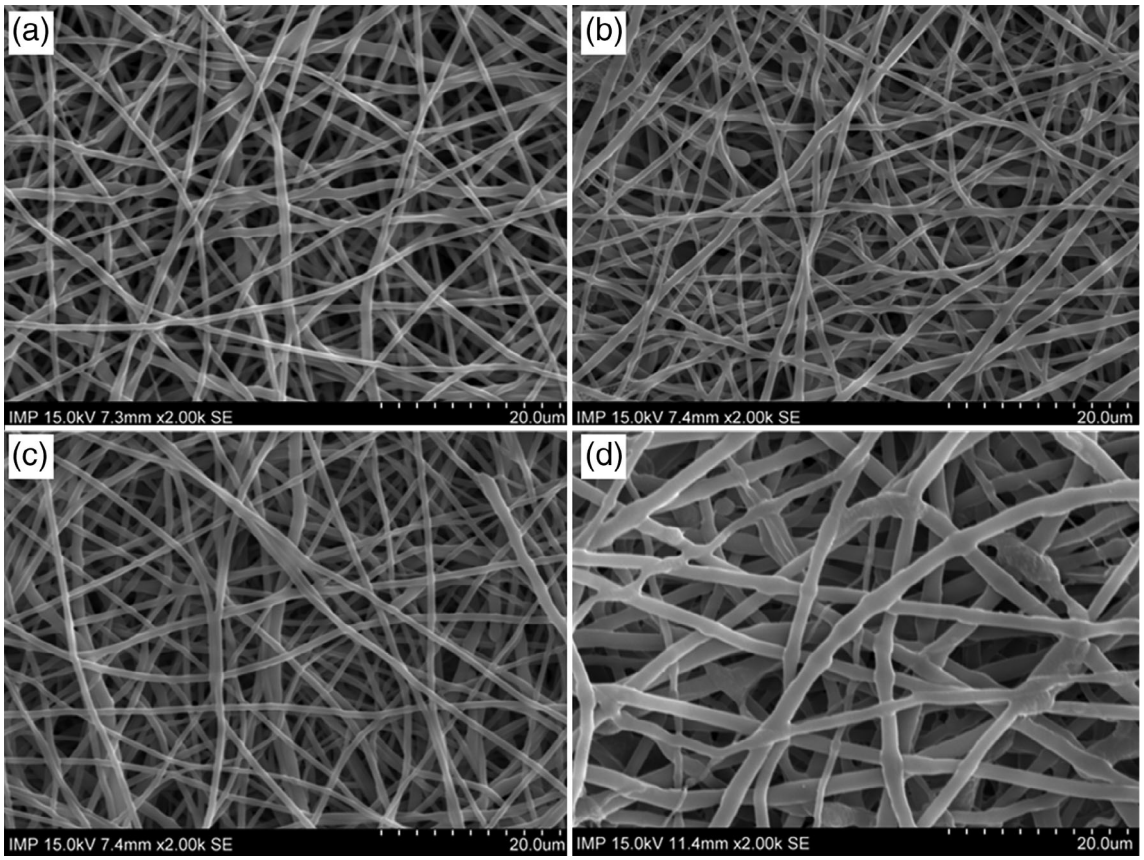

Figure 3. SEM images of electrospun CS-g-PCL/PCL blends. Compositions of the blends (a) 10/90; (b) 40/60; (c) 60/40 days) 90/10.

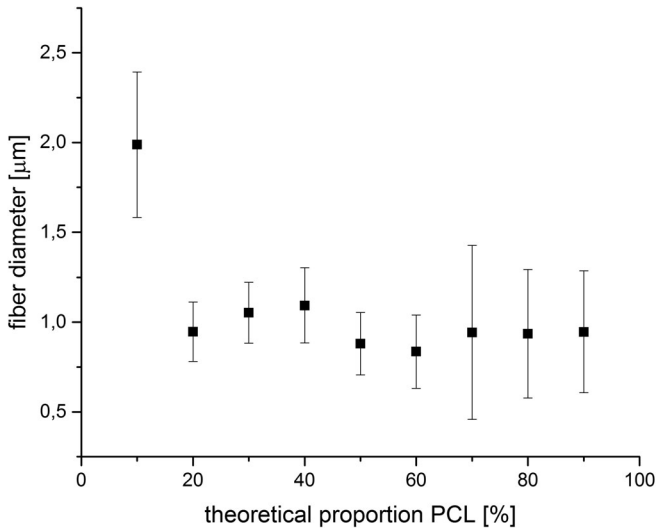

Figure 4. Fiber diameter in [µm] of various PCL blends ($n \geq 100$, SD).

capacity, melting point and glass transition temperature, therefore, were measured. Melting point of samples was determined by using the peak temperature, which was not affected significantly by peak structure or potential peak shoulders. There were no significant changes in melting point (60 ± 1.8 °C) throughout the samples. Besides X-ray diffraction techniques, enthalpy of fusion is the most direct access to measure the degree of crystallinity. The enthalpy of fusion for pure PCL was measured at 54.3 ± 2.0 J/g and for the graft-copolymer CS-g-PCL at 55.8 ± 8.4 J/g. However, electrospinning significantly increased orientation of polymer chains, which fosters the crystallization. Therefore, electrospun PCL showed much higher enthalpy of fusion (72.4 ± 3.3 J/g). The enthalpy of fusion is even higher for electrospun blends of PCL with CS-g-PCL. For a blend composition of 50% (w/w) CS-g-PCL, the enthalpy of fusion was increased to 89.0 ± 1.2 J/g. For a blend with 90% (w/w) CS-g-PCL an enthalpy of fusion of 109.6 ± 1.6 J/g was determined and the material was very brittle. Pure graft-copolymer CS-g-PCL, which was processed by electrospinning showed an enthalpy of fusion of 107.8 ± 2.4 J/g, which was almost double the value for the corresponding but unprocessed graft copolymer. It was concluded that electrospinning led to rearrangement and stretching of polymer chains, which influenced the crystalline properties of the fiber mats. Furthermore, a shoulder with a lower T_m, which indicates smaller crystallites and overall crystallinity can be observed in the recorded thermograms (see Figure 5), which might be induced by the structure of the polymeric graft. It was observed that samples were highly brittle and unusable for further experiments if processed with ≥90% (w/w) of CS-g-PCL.

As calculated by ^{1}H-NMR, the graft copolymer has a composition of 18 PCL units per glucosamine units and consists mainly of PCL units. Using this, the relative fraction of both PCL and

$$\frac{\text{number glucosamine} \times \text{Mw of glucosamine}}{(\text{number glucosamine} \times \text{Mw of glucosamine}) + (\text{number PCL} \times \text{Mw of PCL})} \times 100 = \frac{1 \times 163,82}{(1 \times 163,82 + 18 \times 114,14)} \times 100 = 7.4\% \quad (1)$$

glucosamine can be calculated using their averaged molecular weights and number in the copolymer.

This resulted in a relative fraction of only 7.4 wt% of graft copolymer resulting from glucosamine units and 92.6 wt% resulting from PCL units. Therefore, a rough estimation regarding its crystallinity was made using theoretical value for 100% crystalline PCL. The PCL side chains of CS-g-PCL are short so that they do not show entanglement but due to their high concentration and orientation, which results from the electrospinning process, it is possible that these crystallize better in comparison to pure PCL. This is mainly due to the high orientation, which is caused by electrospinning and stretching on the electrospinning collector. Furthermore, the transition from liquid to solid state during the electrospinning process might enable an enhanced phase separation, which results in regions of pure PCL and regions enriched with Chitosan units. If this is combined with the relatively high surface to volume ratio of electrospun nanofibers this could enable a good and sufficient crystallization process. As shown in Figure 6 an increasing amount of CS-g-PCL in the blend composition led to a higher enthalpy of fusion. To calculate the degree of crystallinity (X_c), the following equation was used,

$$X_c = \frac{\Delta H_F(T_m)}{\Delta H_F^0(T_m^0)} \quad (2)$$

$\Delta H_F(T_m)$ is the measured enthalpy of fusion at the melting point and $\Delta H_F^0(T_m^0)$ is the enthalpy of fusion of completely crystalline PCL $\Delta H_F^0(T_m^0)$. Tiwari and Raj determined $\Delta H_F^0(T_m^0)$ as 139.3 $J \times g^{-1}$.[37] As shown in Figure 6, an increasing amount of CS-g-PCL in the blend led to a significant increase in crystallinity from $X_C = 59\%$ for 10% (w/w) of CS-g-PCL up to $X_C = 78\%$ for 90% (w/w) of CS-g-PCL. Even small amounts of graft copolymer increased crystallinity significantly. This resulted in stiffer fiber mats, which are rather beneficial for the desired mechanical properties of the produced implant. However, it is not beneficial if the fiber mats become too brittle, as seen for samples with a very high content of graft copolymer (≥90 w/w%).

Surface Composition

An important question is whether, and to what extent, the chitosan groups are enriched at the surface of the electrospun fibers of the blends. The chitosan groups are important to improve cell adhesion and allow attachment of nanoparticular drug-delivery systems by electrostatic interaction.[7] To evaluate whether fibers prepared from blends of PCL with CS-g-PCL show an amine-containing surface, fluorescently labeled alginate (Alg-FA) was used. If cationic chitosan amino groups are present at the fiber surface the polyanion Alg-FA will attach to the surface by electrostatic interaction in a simple dipping process.[7] After attaching Alg-FA, all blend compositions showed fluorescence signals even after thorough washing of the fiber mats. The fluorescence intensity scaled with the composition of the blend used for the electrospinning. The higher the amount of CS-g-PCL in the blend, the higher the fluorescence intensity (see Figure 8). To obtain a semiquantitative measure, the sample mean fluorescence intensity was determined using identical CLSM setup and beam intensities. The fluorescence intensity decreased from 1400 ± 300 a.u. (90% (w/w) of CS-g-PCL) to 300 ± 150 (30% (w/w) of CS-g-PCL). A decrease in graft-copolymer content goes along with a decrease in fluorescence intensity. However, this seemed to reach a plateau at 50% (w/w) of graft copolymer. In addition, further decrease in graft-copolymer content did not change fluorescence intensity significantly. Thus, even a small amount of graft copolymer is sufficient to transform the fibers' surface into an active, state, which can be further functionalized. Only high amounts of CS-g-PCL led to a further relevant increase in chitosan groups, and therefore amine functionalities at the fibers' surface.

Table I. Evaluation of electrospun blends consisting of PCL and CS-g-PCL

Theoretical proportion PCL:CS-g-PCL [%]	Measured content PCL [%] ($n \geq 3$)	Contact angle [°] ($n \geq 9$)	Fiber diameter [μm] ($n \geq 100$)	Medium pore size [μm] ($n \geq 3$)
10	12.7 ± 1.3	0	2.04 ± 0.41	Too brittle to be measured
20	30.3 ± 0.8	0	0.95 ± 0.17	2.76 ± 0.24
30	43.4 ± 1.5	0	1.05 ± 0.17	2.55 ± 0.32
40	57.6 ± 0.3	0	1.09 ± 0.21	2.75 ± 0.41
50	63.7 ± 1.8	0	0.88 ± 0.17	2.91 ± 0.26
60	69.2 ± 0.6	0	0.84 ± 0.20	2.69 ± 0.35
70	74.3 ± 1.1	0	0.94 ± 0.48	2.62 ± 0.31
80	85.1 ± 1.0	0	0.93 ± 0.36	2.82 ± 0.42
90	92.3 ± 0.7	0	0.92 ± 0.39	2.45 ± 0.48

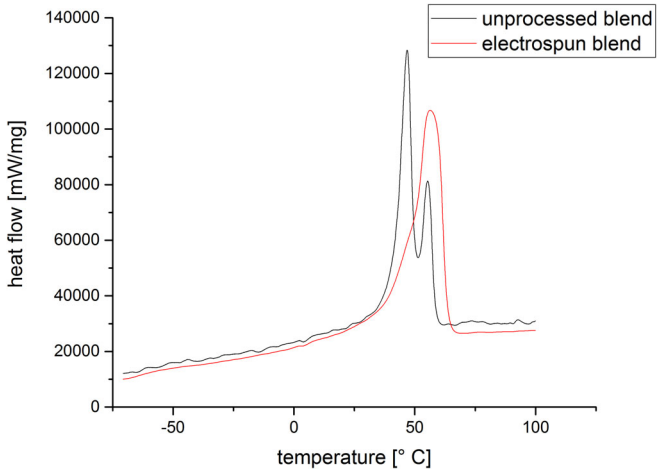

Figure 5. Exemplary thermogram of 40% (w/w) CS-g-PCL with PCL. Shown is the first heat curve. Black curve shows material, which was processed by electrospinning, red curve shows mixed but unprocessed material. [Color figure can be viewed at wileyonlinelibrary.com]

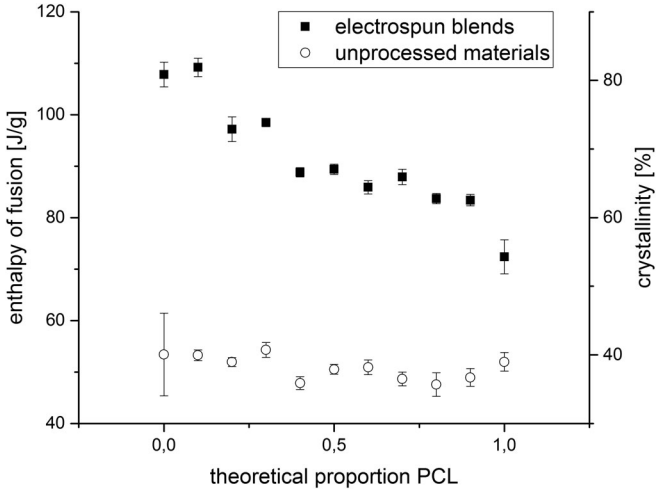

Figure 6. Enthalpy of fusion for electrospun and unprocessed blends of PCL and CS-g-PCL. ($n \geq 3$, SD).

This general increase in fluorescence intensity in conjunction with an increase in graft-copolymer content could be explained by an enrichment of polar functionalities at the fibers' surface. Furthermore, it was observed that fluorescence profiles of the fibers differ depending on their compositions (see Figure 7).

Imaging fibers with high amounts of CS-g-PCL showed homogenous staining with no difference in fluorescence intensity. This has also been observed for fibers with medium amounts of graft-copolymer up to 30% (w/w). This indicates that the graft-copolymer and its amine functionalities, which are necessary for attachment of Alg-FA are present throughout the whole fiber. To achieve this, fibers have to be able to swell to allow the modified biopolymer to pass through and stain the complete fibers, which would be the case if CS-g-PCL is present throughout the whole fiber. For low amounts of graft copolymer, however, it was observed that fluorescence profiles of fibers were no longer homogenous. A hollow pipe-like structure was imaged indicating that amino functionalities of CS-g-PCL were concentrated at the fibers' surface rather than at the fibers' core, resulting in a relative enrichment of the polar amine functionalities at the nonpolar fibers' surface. This observation is commonly known in the literature for other systems,[17] however, could have also been due to a hydrophobic core of the fibers, which did not allow the hydrophilic biopolymer to penetrate into the fibers completely. This possible explanation, however, was rejected based on the XPS results (see below). Taken together, these measurements provide an indirect but quick method to evaluate sample surface functionalities. This experiment also acted as proof of principle to show the versatility and accessibility of the electrospun fiber mats for subsequent functionalization. As we showed in our previous studies, PCL fiber mats modified by crystallizing CS-g-PCL onto the fibers' surface were easily to functionalize by dipping methods.[7] The functionalization with other polymers or drug-delivery systems is based mainly on electrostatic interactions. Since the fibers spun from blends were able to bind a polyanionic polymer, namely alginate, they are accessible to the same functionalization methods as the PCL nanofibers modified by crystallizing CS-g-PCL. Thus, the blending could act as a good alternative, replacing the coating of nanofibers, being less time consuming and a more efficient process.

As CLSM measurements do not give direct access to the actual content of chemical composition of the fiber surface, XPS were carried out. Furthermore, based on its surface sensitivity, XPS can be used to determine whether polar groups, such as chitosan and their amine functionalities, are enriched at the fiber surface.[17] As shown in Figure 8 the nitrogen content determined by XPS was correlated with the actual content of graft copolymer in the blend. There was no good correlation. Even at high PCL content, high N/C ratios were found. The highest values were reached at 50% (w/w) PCL and decreasing for higher amounts of the graftpolymer. Furthermore, we calculated the theoretical nitrogen content for homogenously distributed fibers of the blend compositions used herein. It was seen that theoretical content was significantly lower than measured contents in all cases. Taking into account that XPS is a surface sensitive measurement method with a relatively low penetration depth, this clearly verified the enrichment of polar functionalities at the fiber surface confirming the measured CLSM fluorescence profiles of the fibers.

Cytocompatibility

PCL is known for a compromised biological performance, especially for initial cell attachment.[1,2] In a previous work, we introduced a method for the modification of PCL fiber mats with the graft polymer CS-g-PCL by dip coating and a surface-induced crystallization, which significantly improved the initial cell attachment and viability of the cells.[7] If the surface enrichment of the chitosan in blend fibers would be sufficient to improve the biological performance in a similar way this would be an even easier way to obtain fiber mats for tissue engineering applications. Fiber mats from blends of different compositions were tested for their ability to increase the initial cell attachment and proliferation of MSCs via a viability assay.

Analysis of the cellular dehydrogenase activity was performed with pure PCL fiber mats (100% PCL content) and processed

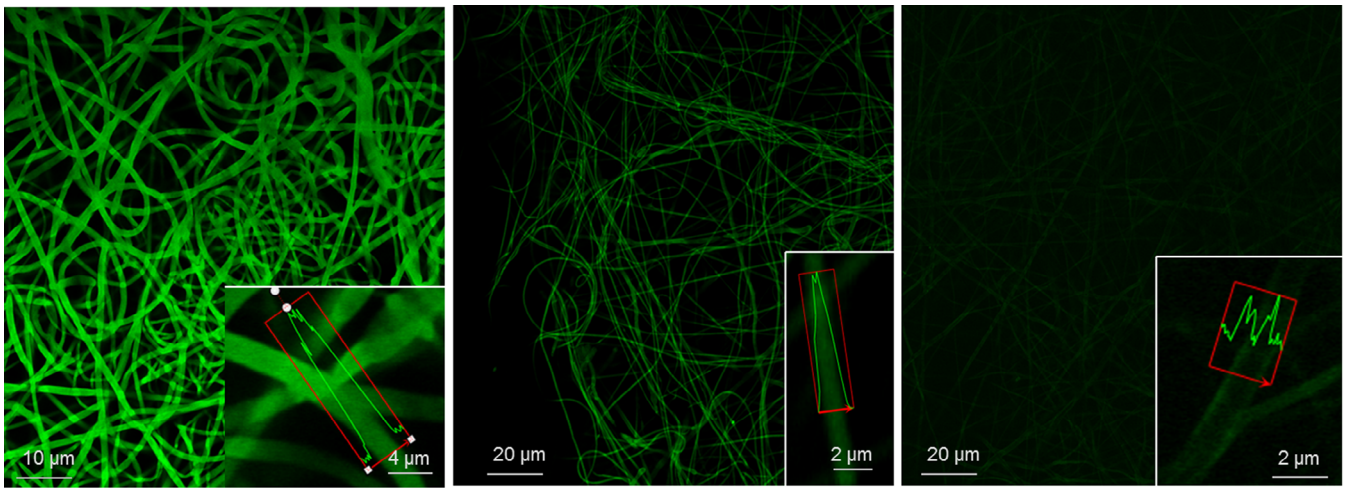

Figure 7. Fluorescence images and profiles for electrospun CS-g-PCL/PCL blends after adsorption of Alg-FA. Composition of the blends (left) 80/20 (middle) 40/60 (right) 20/80. Setup and sensitivity of fluorescence measurements was kept constant to allow for comparison and evaluation of fluorescence intensities. [Color figure can be viewed at wileyonlinelibrary.com]

blends with a CS-g-PCL content ranging from 10 to 80% (w/w) over a time period of 1, 3, and 7 days. Fiber mats with a content of 90% (w/w) of CS-g-PCL were unstable in cell culture media due to their brittleness and therefore could not be tested. Here we show the viability of the cells after 1 day of seeding which reflects the initial cell attachment and the viabilities after 3 and 7 days, which indirectly correspond to the proliferation of the human MSCs (see Figure 9). Short-term cell attachment (1 day) significantly improves with 70–40% PCL content. On the contrary, 90–80% PCL content do not show significant improvement of initial cell attachment but allow better proliferation over time (3–7 days) compared to pure PCL. In general, we observe an increase in vitality from 1 to 7 days for all samples mirroring proliferation of the cells. The viability of the cells is significantly higher under most conditions (90–40% PCL) compared to pure PCL after 7 days of incubation. Our data demonstrate that already 30% (w/w) of CS-g-PCL in the fiber mat is enough to improve initial cell attachment (1 day). The low cell viabilities at low PCL content (<30%) can be explained by the fact that these fiber mats showed a significant decrease in stability and partly even dissociation of the fiber mat in cell culture media. Therefore, the cells are not able to attach properly or rather detach when the fiber mats collapse. In conclusion, it was important to incorporate not more than 60% of CS-g-PCL in the fiber mat. With respect to the initial cell attachment phase

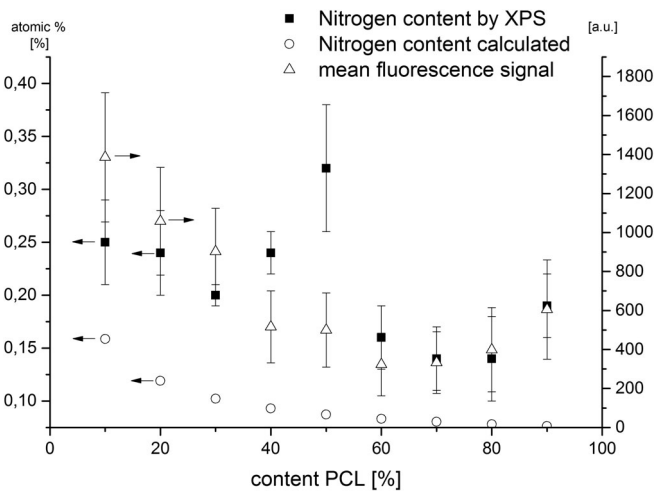

Figure 8. Nitrogen/Carbon (N/C) content of the fibers' surface measured by XPS (black rectangle) in processed blends. One can observe an enrichment of Nitrogen at the fibers' surface compared to the calculated (white circle) values. Data correlates nicely with indirect measurement of active binding sites, in this case amine functionalities, for Alg-FA by CLSM (white triangle, $n = 9$, SD). Arrows indicate the correct axis of ordinates.

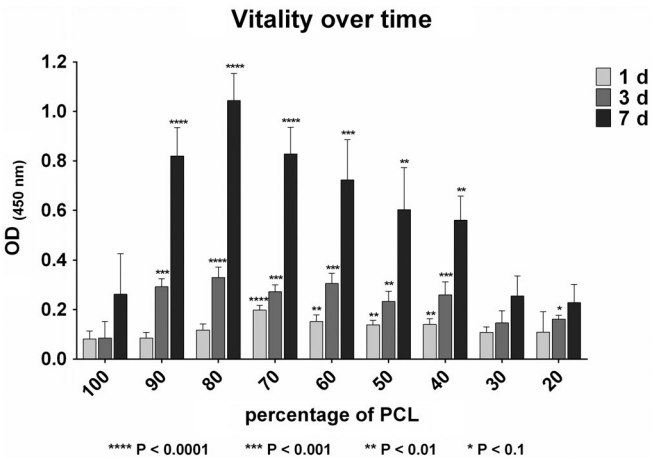

Figure 9. Cytocompatibility testing of processed blends with human MSCs. Viability of the cells was measured via cellular dehydrogenase activity after 1, 3, and 7 days for fiber mats prepared from blends with different contents of PCL. Short-term cell attachment (1 day) significantly improved with 70–40% (w/w) CS-g-PCL content. Long-term viability and proliferation of human MSCs is improved by PCL blends in comparison to pure PCL (3 and 7 days). Statistical significances were analyzed for pure PCL versus PCL blends via student's *t*-test. ****$P < 0.0001$; ***$P < 0.001$; **$P < 0.01$; *$P < 0.1$.

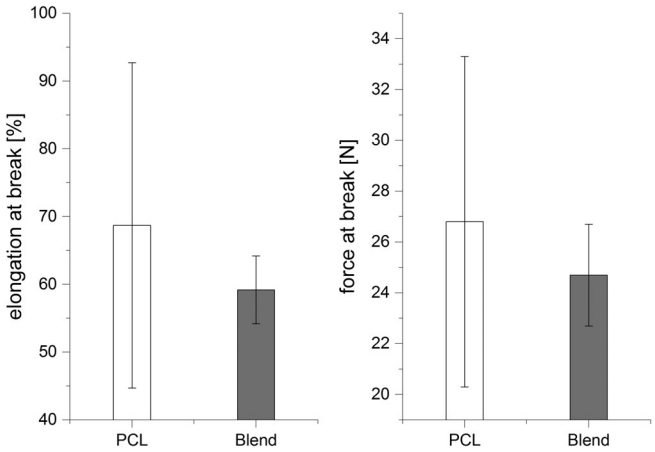

Figure 10. Elongation at break (left) and force at break (right) for pure PCL and PCL:CS-g-PCL blend with a ratio of 60:40 measured at room temperature.

(1 day) and the subsequent proliferation (3–7 days) a content of 30% CS-g-PCL was optimal.

Taking together, blending PCL with CS-g-PCL improved the initial cell attachment and viability of MSCs *in vitro* significantly compared to pure PCL. The results clearly indicate that the surface enrichment of the chitosan groups is sufficient for improved cell compatibility.

Mechanical Properties

Due to its mechanical properties, PCL is already used as a basic implant material. To evaluate if blending CS-g-PCL into electrospun PCL scaffolds does maintain these mechanical properties or weaken the implant, elongation and force at break were measured for pure PCL and CS-g-PCL scaffolds. Since mechanical properties of electrospun fibers are highly depending on the processing parameters used, such as polymer concentration, flow rate, and especially cross section, it is well established that the common comparison of stress and strain is not suitable for these kinds of materials. Therefore, more basic mechanical properties like force at break and elongation at break were investigated for the electrospun fiber mats. The comparison of these parameters is considered to be reliable, provided samples were manufactured using the same protocols.

We used an exemplary composition of 40% (w/w) CS-g-PCL, since this composition showed good surface wettability, sufficient surface charge for subsequent functionalization, and cell compatibility. Due to nature of the electrospun fiber mats, these act differently compared to solid specimens. During load application, the nonaligned fibers are straightened resulting in a high degree of anisotropy, consecutive fiber rearrangement makes a trustworthy recording of forces and elongation complicated. To avoid any corruption of data by rearrangement processes in the material itself, samples were prepared on a rotating drum collector to achieve specimens with aligned fibers.

As shown in Figure 10 the blend was compared to pure PCL regarding its elongation and force at break. Electrospun PCL showed an elongation at break of about 70 ± 23%, while the used blend composition showed no significant difference and reached slightly lower but similar values of 60 ± 7%. The values for force at break of 24 ± 3 N (40% (w/w) CS-g-PCL) is slightly lower compared to 27 ± 5 N (PCL), however due to the relatively large error the difference was not statistically significant. These results indicated that the blend composition used is a promising material to act as a replacement for pure PCL scaffolds. Furthermore, distribution of results and therefore properties, based on the error bars, is narrower for the blends. These results can be compared with published data for native rat tendons, which were determined as maximum force at break for explanted and reimplanted to approximately 28 ± 2 N after full healing period of 8 weeks.[38] This clearly indicated that electrospun PCL/CS-g-PCL blends do have the potential to take up the load present in a rat and therefore, together with its other promising properties such as cytocompatibility, surface wettability, and modifiability, should be tested further in *in vivo* experiments.

CONCLUSIONS

In this work, various blends of CS-g-PCL and PCL were processed to create biocompatible, mechanically strong, and modifiable scaffolds for potential tissue engineering applications. It was shown that processing CS-g-PCL and PCL by electrospinning is possible and the desired proportion could be adjusted during the process. By analyzing SEM images, it was shown that the scaffolds looked similar over a broad range of blend compositions and showed comparable fiber diameters. Interstitial volumes were evaluated as well and showed no significant difference throughout the blends, indicating a very stable electrospinning setup.

Both XPS and CLSM confirmed an increased presence of nitrogen/amine functionalities when adding more graft copolymer. In addition, XPS clearly indicated an enrichment of amine functionalities at the surface compared to theoretically calculated values. This was confirmed by CLSM measurements.

No change in melting point or glass transition temperature was measured by DSC for different blend compositions, however, enthalpy of fusion and therefore crystallinity of the system increased significantly by electrospinning itself. Furthermore, increasing ratios of CS-g-PCL led to a higher enthalpy of fusion of up to 110 J/g for 90% (w/w). This might be due to a rearrangement of the polymer chains and therefore increased ability to form crystalline regions.

Blends showed a significantly increased cytocompatibility for human primary cells. It was shown that minor amounts of CS-g-PCL are sufficient to improve initial cell attachment and proliferation, while very high concentrations of CS-g-PCL, which resulted in rigid and unstable fiber mats, are not beneficial. Furthermore we analyzed an exemplary blend composition regarding its mechanical properties, which are similar to electrospun PCL fiber mats.

We conclude that blending CS-g-PCL with PCL is a promising approach to act as an alternative for PCL fiber mats coated with CS-g-PCL[7] and to act as scaffolds suitable for *in vivo* tissue engineering applications.

REFERENCES

1. Font Tellado, S.; Balmayor, E. R.; van Griensven, M. *Adv. Drug Deliv. Rev.* **2015**, *94*, 126.

2. Hutmacher, D. W. *Biomaterials*. **2000**, *21*, 2529.
3. Ma, G.; Song, C.; Sun, H.; Yang, J.; Leng, X. *Contraception*. **2006**, *74*, 141.
4. Müller, M. Faserbasierte abbaubare kardiovaskuläre Gefäßprothesen: Entwicklung; Herstellung und Prüfung: Garbsen, TEWISS Verlag, **2018**.
5. Bode, M.; Mueller, M.; Zernetsch, H.; Glasmacher, B. *Current Directions Biomed Eng.* **2015**, *1*, 459.
6. Szentivanyi, A.; Chakradeo, T.; Zernetsch, H.; Glasmacher, B. *Adv. Drug Deliv. Rev.* **2011**, *63*, 209.
7. de Cassan, D.; Sydow, S.; Schmidt, N.; Behrens, P.; Roger, Y.; Hoffmann, A.; Hoheisel, A. L.; Glasmacher, B.; Hänsch, R.; Menzel, H. *Colloids Surf. B Biointerfaces*. **2018**, *163*, 309.
8. Nair, L. S.; Laurencin, C. T. *Prog. Polym. Sci.* **2007**, *32*, 762.
9. Fu, X.; Sammons, R. L.; Bertóti, I.; Jenkins, M. J.; Dong, H. *J. Biomed. Mater. Res. B Appl. Biomater.* **2012**, *100*, 314.
10. Tallawi, M.; Rosellini, E.; Barbani, N.; Cascone, M. G.; Rai, R.; Saint-Pierre, G.; Boccaccini, A. R. *J. R. Soc. Interface*. **2015**, *12*, 20150254.
11. Cui, W.; Zhou, Y.; Chang, J. *Science Technol Adv Mater.* **2010**, *11*, 014108.
12. Gunn, J.; Zhang, M. *Trends Biotechnol.* **2010**, *28*, 189.
13. a) Zhou, Y.; Yang, D.; Chen, X.; Xu, Q.; Lu, F.; Nie, J. *Biomacromolecules*. **2008**, *9*, 349. b) Khor, E.; Lim, L. Y. *Biomaterials*. **2003**, *24*, 2339.
14. a) Jayakumar, R.; Prabaharan, M.; Muzzarelli, R. A. A., Eds. Chitosan for Biomaterials II; Springer Berlin Heidelberg: Berlin, Heidelberg, **2011**. b) Leedy, M. R.; Martin, H. J.; Norowski, P. A.; Jennings, J. A.; Haggard, W. O.; Bumgardner, J. D. Use of chitosan as a bioactive implant coating for bone-implant applications. In Chitosan for Biomaterials II, Springer Berlin Heidelberg: Berlin, Heidelberg, **2011**. p. 129.
15. Chen, H.; Huang, J.; Yu, J.; Liu, S.; Gu, P. *Int. J. Biol. Macromol.* **2011**, *48*, 13.
16. Jing, X.; Mi, H.-Y.; Wang, X.-C.; Peng, X.-F.; Turng, L.-S. *ACS Appl. Mater. Interfaces*. **2015**, *7*, 6955.
17. van Royen, P.; Boschmans, B.; dos Santos, A.; Schacht, E.; Dubruel, P.; Cornelissen, R.; Beenaerts, L.; van Vaeck, L. *Anal. Bioanal. Chem.* **2011**, *399*, 1163.
18. Seyednejad, H.; Ji, W.; Yang, F.; van Nostrum, C. F.; Vermonden, T.; van den Beucken, J. J. J. P.; Dhert, W. J. A.; Hennink, W. E.; Jansen, J. A. *Biomacromolecules*. **2012**, *13*, 3650.
19. Prabhakaran, M. P.; Venugopal, J. R.; Chyan, T. T.; Hai, L. B.; Chan, C. K.; Lim, A. Y.; Ramakrishna, S. *Tissue Eng. Part A*. **2008**, *14*, 1787.
20. a) van der Schueren, L.; Steyaert, I.; de Schoenmaker, B.; de Clerck, K. *Carbohydr. Polym.* **2012**, *88*, 1221. b) Bai, H.; Huang, C.; Xiu, H.; Zhang, Q.; Deng, H.; Wang, K.; Chen, F.; Fu, Q. *Biomacromolecules*. **2014**, *15*, 1507.
21. Zernetsch, H.; Repanas, A.; Rittinghaus, T.; Mueller, M.; Alfred, I.; Glasmacher, B. *Fibers Polym.* **2016**, *17*, 1025.
22. Sydow, S.; de Cassan, D.; Hänsch, R.; Gengenbach, T. R.; Easton, C. D.; Thissen, H.; Menzel, H. *Biomater. Sci.* **2018**, *7*, 233.
23. Schindler, C.; Williams, B. L.; Patel, H. N.; Thomas, V.; Dean, D. R. *Polymer*. **2013**, *54*, 6824.
24. Sarasam, A. R.; Krishnaswamy, R. K.; Madihally, S. V. *Biomacromolecules*. **2006**, *7*, 1131.
25. Markovic, G.; Visakh, P. M. Polymer blends. In Recent Developments in Polymer Macro, Micro and Nano Blends, Woodhead Publishing: Sawston, UK, **2017**. p. 1.
26. Chun, D. H. R. a. I. *Nanotechnology*. **1996**, *7*, 216.
27. Qin, X. Coaxial electrospinning of nanofibers. In Electrospun Nanofibers, Woodhead Publishing: Sawston, UK, **2017**. p. 41.
28. a) Martina, M.; Hutmacher, D. W. *Polym. Int.* **2007**, *56*, 146. b) Cipitria, A.; Skelton, A.; Dargaville, T. R.; Dalton, P. D.; Hutmacher, D. W. *J. Mater. Chem.* **2011**, *21*, 9419.
29. Zhu, Y.; Gao, C.; Liu, X.; Shen, J. *Biomacromolecules*. **2002**, *3*, 1312.
30. Li, Y.; Ceylan, M.; Shrestha, B.; Wang, H.; Lu, Q. R.; Asmatulu, R.; Yao, L. *Biomacromolecules*. **2014**, *15*, 319.
31. Wenzel, R. N. *Ind. Eng. Chem.* **1936**, *28*, 988.
32. Tamada, Y.; Ikada, Y. *J. Colloid Interface Sci.* **1993**, *155*, 334.
33. de Cassan, D.; Hoheisel, A. L.; Glasmacher, B.; Menzel, H. *J. Mater. Sci. Mater. Med.* **2019**, *30*, 42.
34. Sarath, C. C.; Shanks, R. A.; Thomas, S. Polymer Blends. In Nanostructured Polymer Blends, William Andrew Publishing: Norwich NY, **2014**. p. 1.
35. Wu, X.; Chen, J.; Zeng, X. *Angew. Makromol. Chemie.* **1991**, *189*, 183.
36. Rim, P. B.; Runt, J. P. *Macromolecules*. **1983**, *16*, 762.
37. Tiwari, A.; Raj, B. Reactions and Mechanisms in Thermal Analysis of Advanced Materials; John Wiley & Sons; Scrivener Publishing: Hoboken, New Jersey, Salem, Massachusetts, **2015**.
38. You, X.; Shen, Y.; Yu, W.; He, Y. *Mol. Med. Rep.* **2018**, *17*, 4981.